

# Optimization of the optical properties of Safranin O –Polycarbonate composites for Algae Greenhouse Applications

N. Hendawy, , A. Bakr, T. Y. Elrasasi \*

Department of Physics, Faculty of science, Benha University, Egypt

## Abstract

Safranin O/ Polycarbonate composite layers were prepared by solution-casting method. The optical absorption of Safranin O -Polycarbonate composite was studied in the range (400-1100 nm) for different concentrations of Safranin O from 50ppm up to 250ppm. It showed absorption characteristic peak at 518 nm which increased with dye concentration. The detection of fluorescence of polymer composite illustrated a fluorescence peak from 564 nm up to 589 nm with maximum intensity at 50ppm. The polymer composites were characterized by using DSC, TGA, and FT-IR which did not illustrate any structure variation with the addition of Safranin O dye up to 250 ppm. Bulk conductivity and dielectric parameters were studied also.

**Keywords:** Polycarbonate; Safranin O; Fluorescent polymer composite; Algae biofuel.

## 1. Introduction

Recently, polymer composites have attracted the attention of scientists due to their wide and attractive different properties e.g. easy manufacturing, weathering durability, light weight and good optical and mechanical properties [1]. Polymer composites can be used in numerous modern applications, such as organic solar cells, thermal and photo solar collectors, displaying, semiconductors and greenhouses applications. The greenhouse applications such as planting, vegetables and fruits drying and desalination need suitable polymeric film for covering the greenhouse to create a good environment conditions. The polymeric film should be transparent, has good mechanical properties, good UV resistance degradation, and thermal stability [2].

---

Many polymers are used in the greenhouse applications such as clear polyvinyl chloride (PVC), Polymethyl methacrylate (PMMA), Polycarbonate (PC), Polyethylene (PE), and Polypropylene (PP)[3]. PE and PP are used because of their lowcost and good mechanicalproperties [4]. On the other hand, PMMA and PC are used because of their perfect optical properties [5].

PC is one of the most thermoplastic polymers used in the greenhouse applications because it is often colorless, high transmission to the visible light up to 90%, high refractive index (1.588) and densitylowerthan most types of glasses (1.52 g/cm<sup>3</sup>)[6].

Fluorescent polymer composites (FPCs) which used in greenhouse applications are consists of a suitable transparent polymer doped with anorganic or inorganic fluorescent material. FPCsare used to convert the unused solar spectra intofavorable spectrawhich can increase the performance in the greenhouseapplications.

Safranine O fluorescent organic dye is used in FPCs because it has emission peak in the range of optical absorption spectra of algae.

The aim of this work is preparation of PC doped with Safranine O dye emitting photons in the range of optical absorption spectra of algae (chlorophyll B) to be used in algae biodiesel production. The optical absorption and fluorescenceof all dye-polymer composites are analyzed in detail. In addition, the quantum efficiency spectra of the prepared films have been presented. Besides, different thermal analyses of the FPCs werestudiedto examine the thermal stability of the polymer composites.

## **2. Experimental**

### **2.1. Material processing**

PC was provided by Styron Europe, Germany, which have excellent transparency, high heat resistance [6].Safranine O fluorescent dye was provided by Loba Chemie Pvt.Itd. Mumbai, India. In addition, dichloromethane (CH<sub>2</sub>CL<sub>2</sub>) was used as a common solvent for PC and Safranine O as well.

Safranine O -polycarbonate composite films were prepared by solution-casting method. PC and Safranine O were dissolved in dichloromethane and stirred for 30 min at room temperature. After that, Safranine O was added to PC solution atdifferent

concentrations from 50 ppm up to 250 ppm (concentrations were calculated by solid PC/solid dye). Then, the samples (Safranin O -PC) were casted in Petri-glass dishes and left at 70 °C for (35) min to get a completely dry.

## 2.2. Sample characterization

The absorption spectra of the prepared films were investigated in the wavelength range (190-1100 nm) using a UV-VIS spectrophotometer JENWAY 6405 UV/VIS Spectrophotometer. Fluorescent properties of the prepared films were investigated by rf-5301 pc spectrofluorophotometer, Shimadzu, 150W Xenon lamp, wavelength range (220-900nm). FT-IR spectra were examined by using 6300 Fourier transform infrared spectrometer in the wave number range (400-4000  $\text{cm}^{-1}$ ). Thermo-gravimetric (TGA) data were obtained by using Shimadzu thermal analyzer system at a heating rate of 20°C/min, under  $\text{N}_2$  (20ml/min) flow in the range from room temperature up to 600°C. Thermo-analytical data were obtained by using PerkinElmer DSC-7 power compensation differential scanning calorimeter. Finally, dielectric parameters and electrical measurements were carried out in the room temperature using pm 6304 programmable automatic (RLC Philips meter). The measurements were carried out over a frequency range 100 Hz to 100 kHz.

## 3. Results and discussion

### 3.1. Optical absorption

The absorption spectra for all Safranin O -PC composite films are shown in Fig.3.1, which illustrates absorption band around 518 nm. One can see that the maximum absorption wavelength ( $\lambda_m$ ) for all concentrations is 518 nm i.e. at the blue-yellow optical band. Moreover, as shown in Fig.3.2, the area under the absorption curves and the absorption intensity increases by increasing the dye concentration, this can be attributed to the increase of absorbing dye molecules.

The absorbance  $A$  can be explained by Lambert-Beer's law, Eq. (3.1)

$$A = C d \alpha (\lambda) \quad (3.1)$$

where  $C$  is the dye concentration,  $d$  is the thickness and  $\alpha$  is the absorption coefficient.

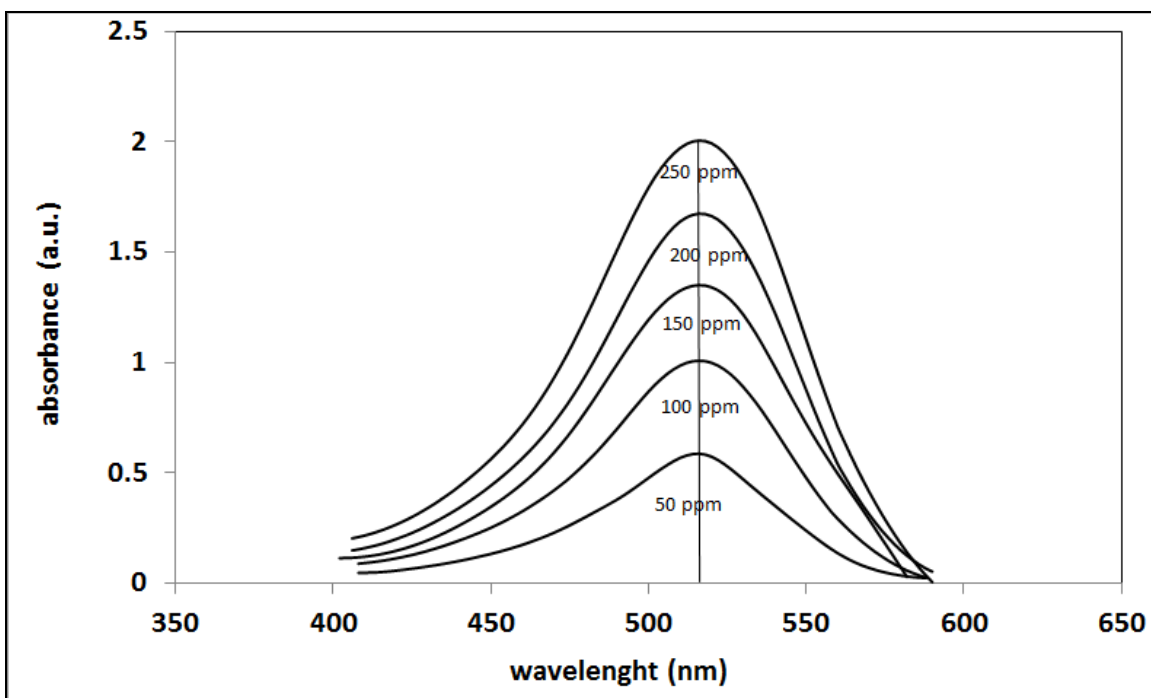


Fig.3.1 The absorption spectra of Safranin O -PC composites at different concentrations.

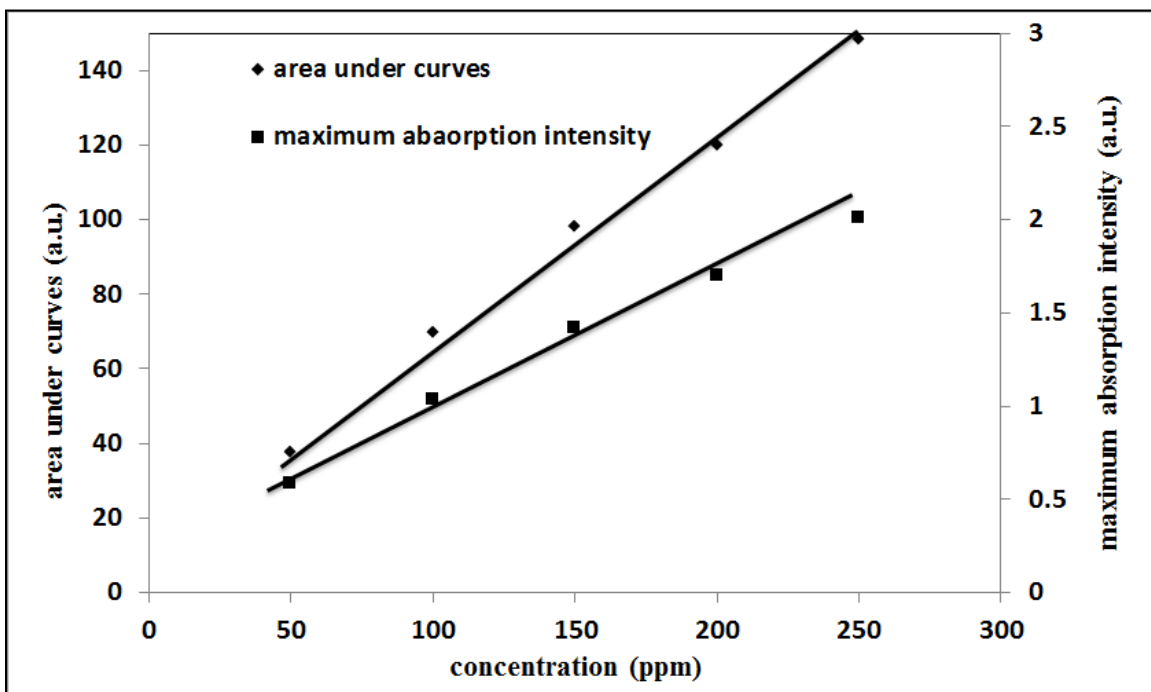


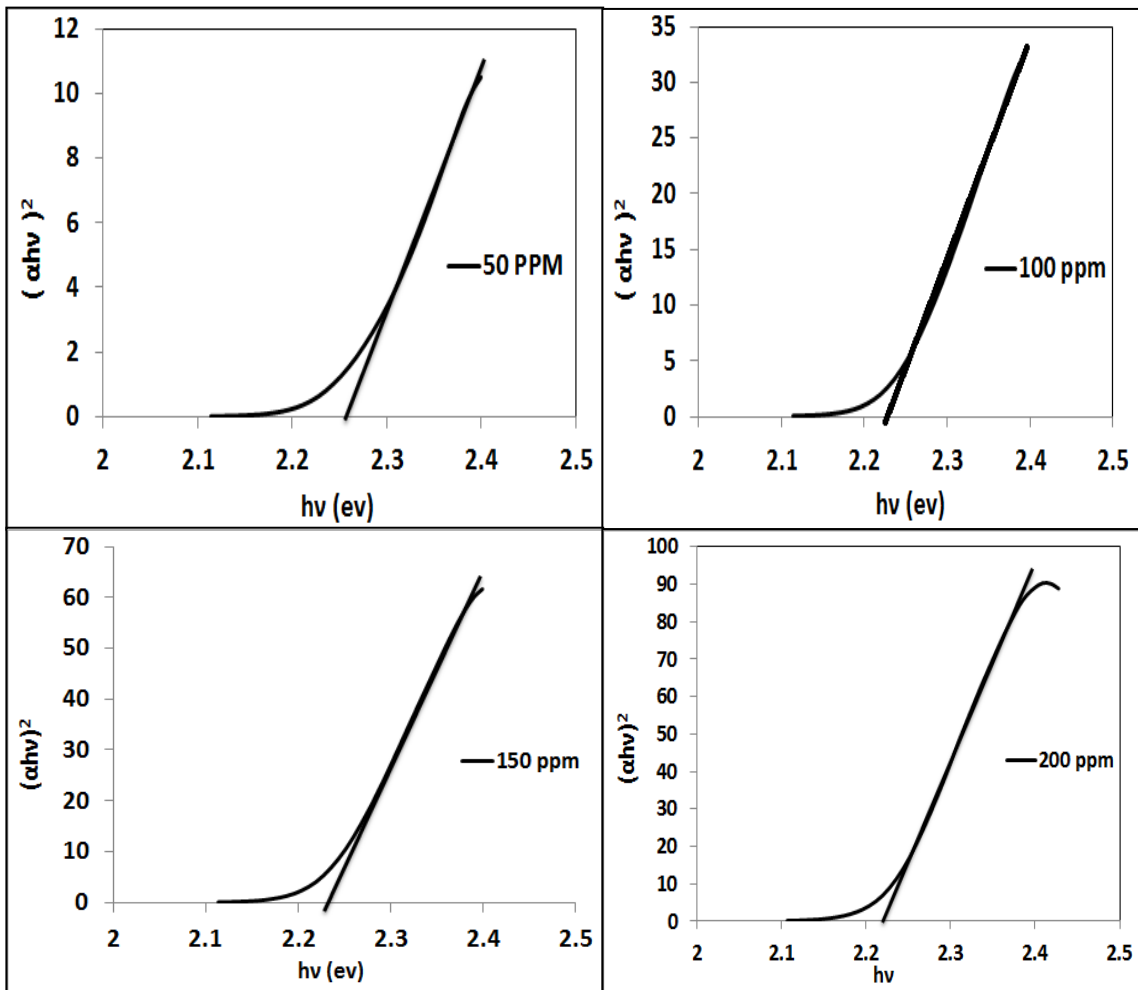
Fig. 3.2 Area under absorption curves and maximum absorption intensity of Safranin O -PC composites at different concentrations.

### 3.2. Optical Band Gaps ( $E_g$ )

The electronic transitions are the essential parameter of the optical absorption. These transitions are controlled by certain selection rules, which can be expressed by Eq. (3.2).

$$\alpha h\nu = A (h\nu - E_g)^n \quad (3.2)$$

where  $h\nu$  is the photon energy,  $\alpha$  is the absorption coefficient,  $A$  is a constant, and  $n$  is a constant with allowed values of  $1/2$  and  $2$  and not allowed values of  $3/2$  and  $3$  for direct and indirect transitions respectively [7]. To ascertain the transition mode,  $n$  has been obtained using the first derivative of Eq. (3.2) and absorption data, it is in the range (0.839-0.987) which predicts the electronic allowed direct transition. To determine the direct optical energy gap, the  $\alpha h\nu^2$  was plotted vs.  $h\nu$  for all concentrations as shown in Fig.3.3.



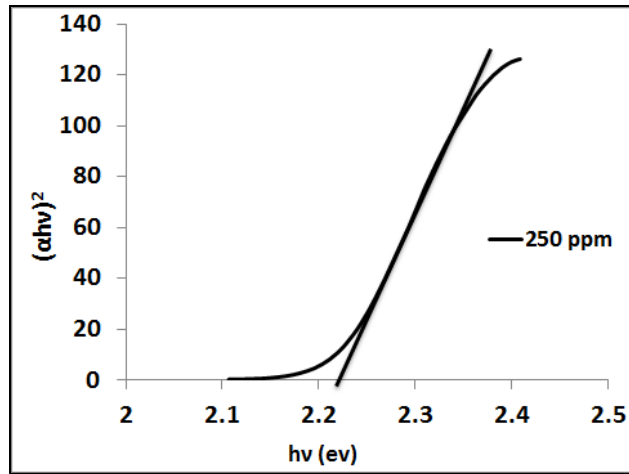


Fig.3.3  $h\nu$  vs.  $\alpha h\nu^2$  of Safranine O –PC composites at different concentrations.

The values of the direct inter band transition were estimated from the intercept of the energy axis as listed in Table 3.1 [8]. Table 3.1 shows that the energy gap of Safranine O -PC composites decreased slightly with increasing concentration due to the change in the morphology of the band structure [9].

### 3.3. Optical fluorescence

The fluorescence spectra for all Safranine O -PC composites are shown in Fig. 3.4 at which when concentration increased, maximum fluorescence wavelength increased from (564-589) nm that also due to the change in the morphology of the band structure [9]. The maximum fluorescence intensity and the area under the fluorescence curves decreased with increasing Safranine O concentration from 50 ppm up to 250 ppm, see Fig. 3.5.

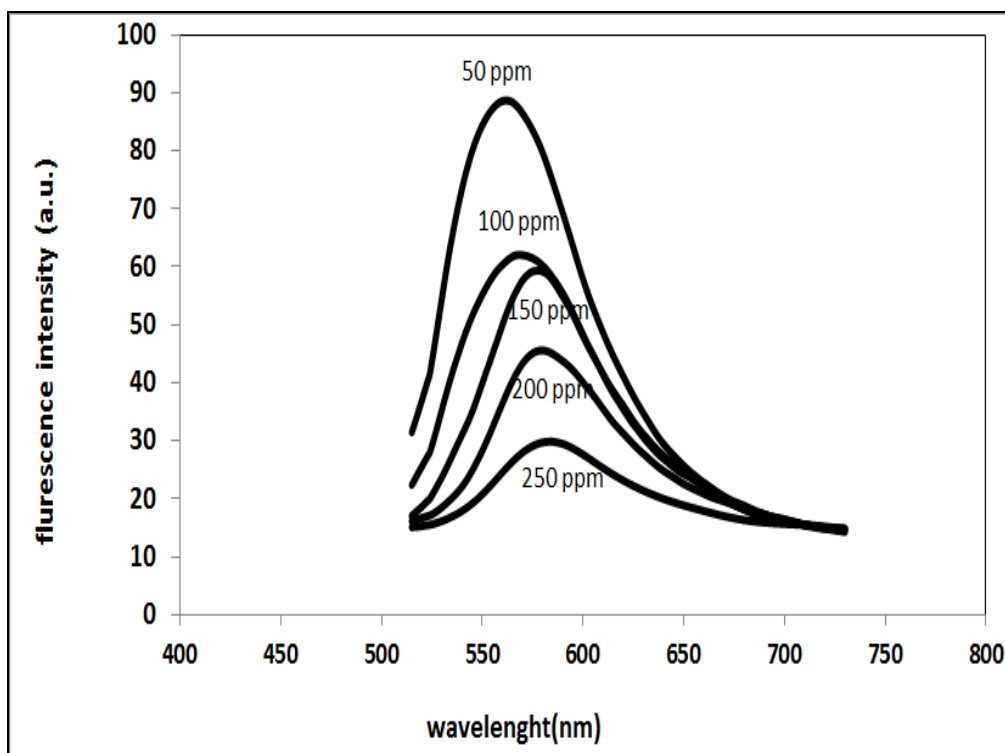


Fig. 3.4 The fluorescence spectra of Safranin O –PC composites at different concentrations.

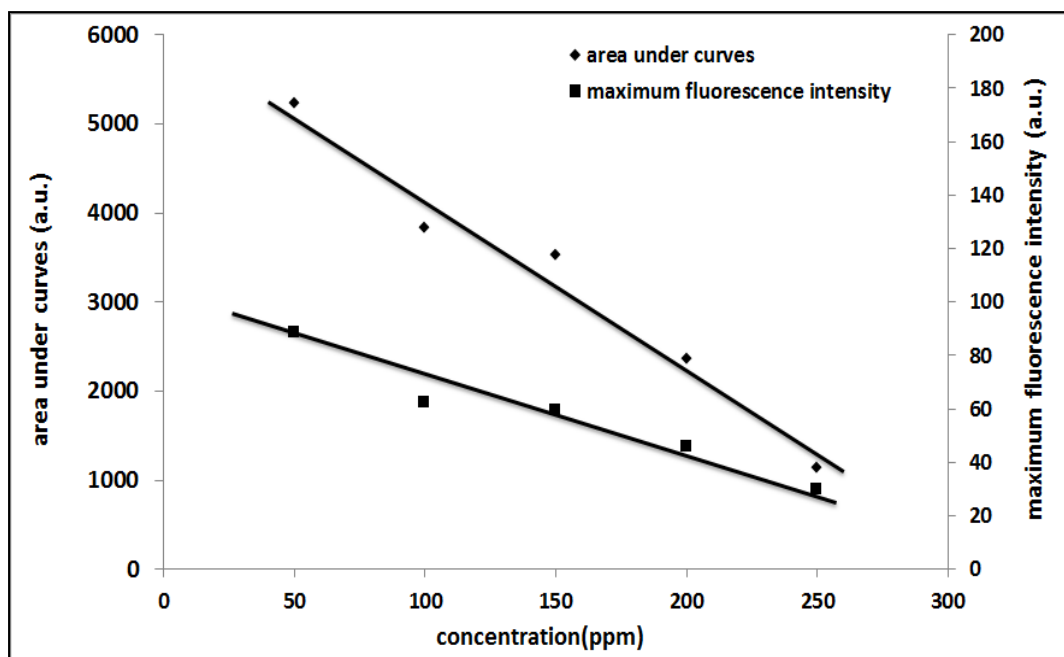


Fig. 3.5 Area under fluorescence curves and maximum fluorescence intensity of Safranin O -PC composites at different concentrations.

### 3.4. Optical Quantum efficiency

The optical quantum efficiency ( $\phi$ ) is defined as the ratio of emitted photons to the absorbed photons [10], which is proportional to the area under fluorescence  $A_{flu}$  curves to the area under absorption curves  $A_{abs}$  neglecting the scattered and reflected photons, see Eq.(3.3).

$$\phi = \frac{\text{no of emitted photons}}{\text{no of absorbed photons}}$$
$$\frac{\text{no of emitted photons}}{\text{no of absorbed photons}} \sim \frac{A_{flu}}{A_{abs}} = B \quad (3.3)$$

The ratio  $A_{flu} / A_{abs} = B$  has been obtained by using the absorption and fluorescence curves at different concentrations of Safranin O in PC polymer matrix. Fig. 3.6 shows quantum yield  $B$  vs. Safranin O concentration, one can see that,  $B$  decreases by increasing the concentration of Safranin O, due to the decreasing of area under fluorescence curve with increasing concentration.

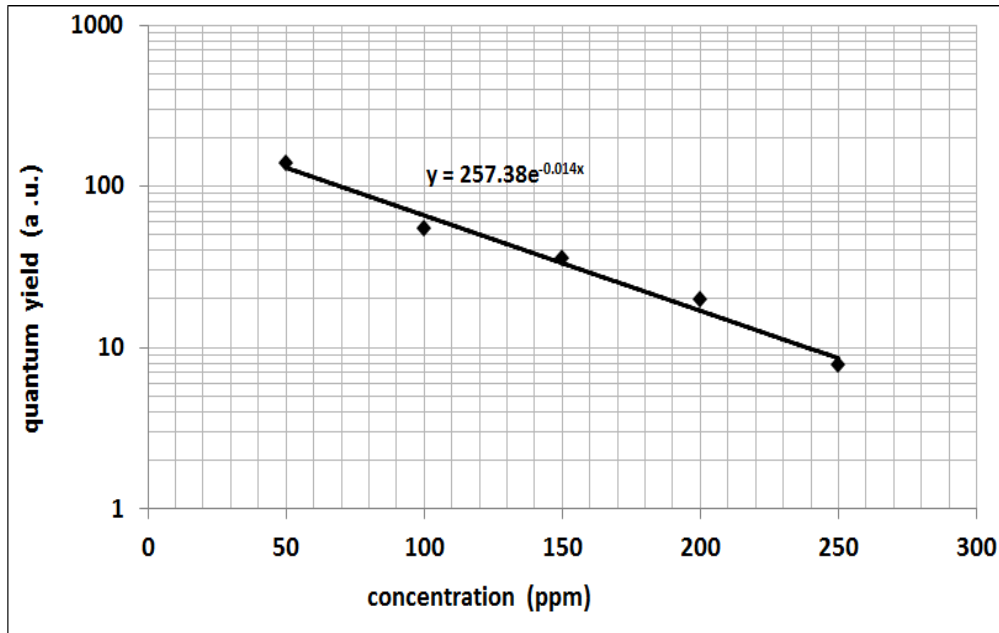


Fig. 3.6 Quantum yield of Safranin O -PC composites at different concentrations.



**Table 3.1 Optical parameters of Safranine O –PC composites at different concentrations.**

<b>Concentration (ppm)</b>	<b>Area under absorption curve(a.u.)</b>	<b>Area under fluorescence curve (a.u.)</b>	<b>Maximum absorption intensity (a.u.)</b>	<b>Maximum fluorescence intensity (a.u.)</b>	<b>E<sub>g</sub> (ev)</b>
<b>50 ppm</b>	<b>37.667</b>	<b>5227</b>	<b>0.586</b>	<b>88.674</b>	<b>2.26</b>
<b>100 ppm</b>	<b>69.579</b>	<b>3829</b>	<b>1.037</b>	<b>62.05</b>	<b>2.24</b>
<b>150 ppm</b>	<b>98.174</b>	<b>3523</b>	<b>1.414</b>	<b>59.322</b>	<b>2.23</b>
<b>200 ppm</b>	<b>120.124</b>	<b>2363</b>	<b>1.698</b>	<b>45.57</b>	<b>2.225</b>
<b>250 ppm</b>	<b>148.35</b>	<b>1146</b>	<b>2.008</b>	<b>29.841</b>	<b>2.22</b>

### **3.5. FT-IR Spectroscopy**

Fig. 3.7 shows the FT-IR spectra of Safranine O -PC composites with different concentrations of Safranine O (50, 150 and 250 ppm). The absorption peaks can be detected for all concentrations as listed in Table 3.2 [11]. From the FT-IR spectra of Safranine O –PC composites, there is no effect of dye concentration on the chemical bonds inside polymer.

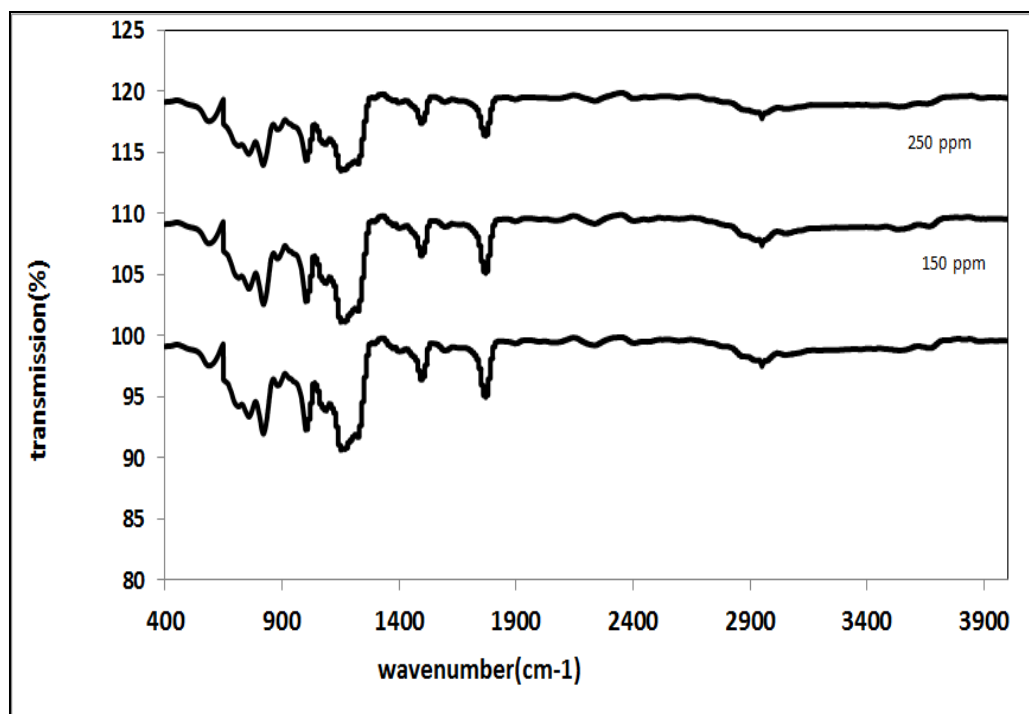


Fig. 3.7 FT-IR spectrum of Safranin O –PC composites at different concentrations .

**Table 3.2 FT-IR absorption bands of Safranin O -PC composites at different concentrations.**

Wavenumber(cm) <sup>-1</sup>	Assignment	50 ppm	150 ppm	250 ppm
2972	(C-H) stretching, Aromatic	2970.09	2974.11	2973.31
1780	(C=O) stretching, Ketone	1784.04	1781.23	1780.89
1501	(C=C) stretching, Aromatic	1504.85	1501.21	1504.67
1189	(C-O) stretching, Ether	1185.95	1189	1194
1004	(C-O) stretching, Ether	1002.41	1004.25	1001.10
554	(CH <sub>2</sub> ) <sub>n</sub> , Alkane	554	554.31	554

### 3.6. Thermo gravimetric Analysis (TGA)

The thermal stability for Safranin O -PC composites at different concentrations has been studied by using TGA technique as shown in Fig. 3.8. One can see that Safranin O -PC composites have thermal stability up to 370 °C. Above that temperature we get PC composites degradation. That degradation is due to chemical interaction between carbonate groups and residual traces of water and hydroxy-groups, followed by gases release (CO<sub>2</sub>, CH<sub>4</sub>, CO) [12].

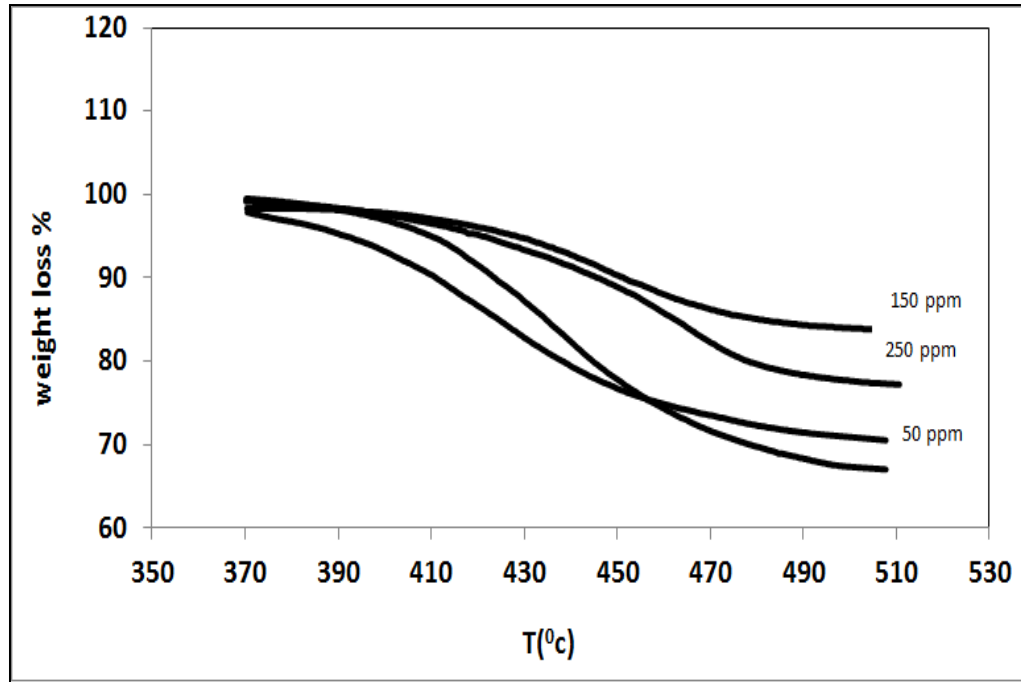


Fig.3.8 Weight loss of Safranin O -PC composites at different concentrations vs. Temperature.

The thermal decomposition and subsequent weight loss of the solid can be expressed by the following reaction rate equation (coats equation) [13],

$$\frac{d\alpha}{dt} = k(1 - \alpha)^n \quad (3.5)$$

where  $\alpha = \frac{w_i - w_t}{w_i - w_f}$  is the loss fraction,  $w_i$ ,  $w_f$  are the initial weight and final weight respectively,  $w_t$  is the weight at given temperature,  $n$  is the reaction order takes the values 1 to 4 and  $k$  is the reaction rate constant, which represented by Arrhenius equation,

$$k = A e^{-E/RT} \quad (3.6)$$

where  $R$  is the universal gas constant,  $E$  is the decomposition energy,  $T$  is the absolute temperature and  $A$  is the frequency factor. The degradation kinetics ( $n = 1$ ) of the presented PC with different concentrations of Safranin O can be expressed by the following relation,

$$\log \left[ \frac{-\log(1-\alpha)}{T^2} \right] = \log \left[ \frac{\left(1 - \frac{2RT}{E}\right) AR}{\beta E} \right] - \frac{E}{2.303RT} \quad (3.7)$$

The values of  $E$  have been extracted using the least square fitting of Eq. (3.7), and listed in Table 3.3 where  $\beta$  is the heating rate. It's clear that, perylene did not affect the thermal stability of PC.

### 3.7. Differential scanning calorimetric (DSC)

Fig. 3.9 shows the DSC thermo-grams for Safranin O –PC composite at different concentrations of Safranin O dye. Two endothermic peaks appear, the first around 82°C and the second around 287°C refer to the glass transition temperature,  $T_g$  and melting temperature,  $T_m$  respectively for selected concentrations of Safranin O up to 250 ppm, as listed in Table 3.3.

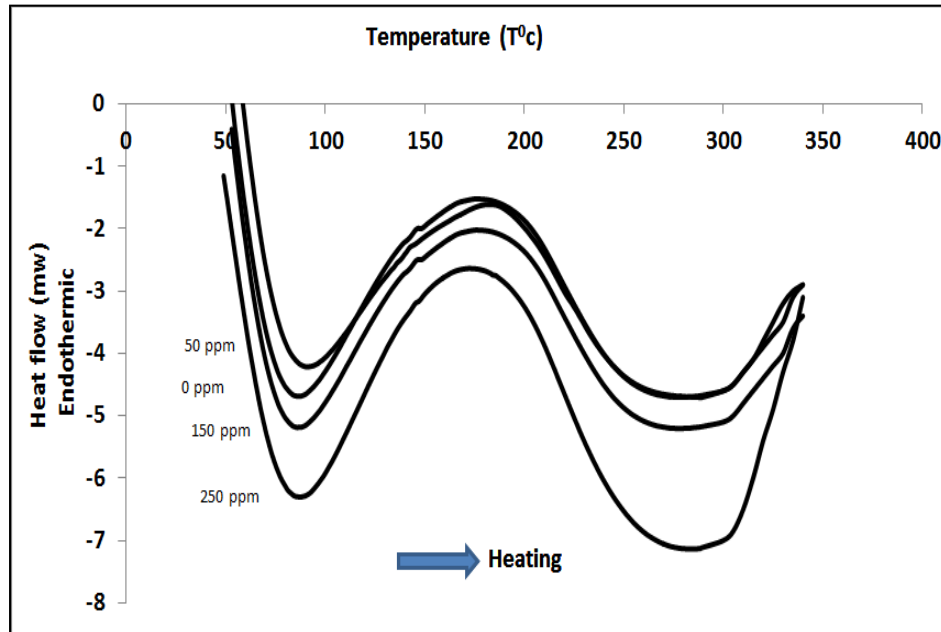


Fig. 3.9 DSC results of Safranin O -PC composite at different concentrations.

It is clear that, no change of the position of both glass transition temperature and melting temperature, this confirms that no chemical interaction between dye and polycarbonate.

**Table 3.3 Thermal parameters of Safranin O –PC composites at different concentrations.**

Concentration (ppm)	Glass transition temperature( <sup>0</sup> c)	Melting temperature ( <sup>0</sup> c)	Decomposition energy (kj/mole)
0	80.3	288	165.351
50	82.89	288.14	165.638
150	82.44	288.14	166.098
250	83.23	287.58	165.92

### 3.8. Complex impedance spectroscopy

#### 3.8.1. Bulk conductivity

The complex impedance analysis method was used to determine the bulk electrical conductivity  $\sigma_b$  of all samples. The impedance was analyzed to a real part  $Z'$  and imaginary part  $Z''$  on the complex plane at room temperature for Safranin O -PC composites as shown in Fig. 3.10. The impedance plot, in general, shows a semicircle its center is below the  $Z'$  axis where the semicircle reflects the impedance of charge transfer. The intersection with  $Z'$  axis represents the sample bulk resistance  $R_b$  at high frequency region. The values of bulk conductivity  $\sigma_b$  of the polymer composites were obtained by Eq. (3.8) [14].

$$\sigma_b = d/R_b A \quad (3.8)$$

where  $d$  is the sample thickness and  $A$  is its effective area for different concentrations of polymer composite.

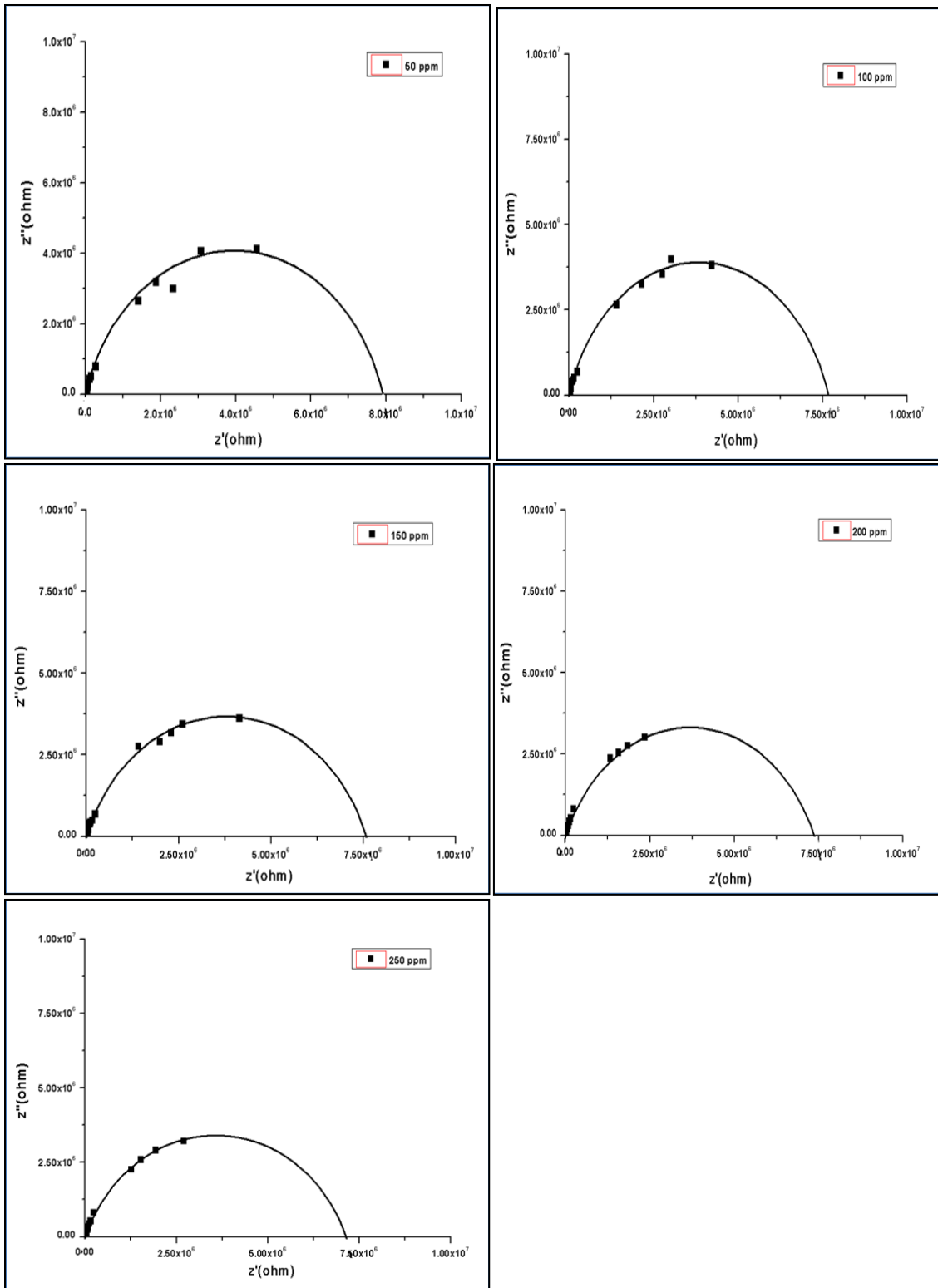


Fig. 3.10 The impedance plot of the imaginary part  $Z''$  against the real part  $Z'$  at room temperature at different concentration.

As listed in table 3.4, we founded that bulk conductivity of Safranine O –PC composite at different concentrations did not changed.

**Table 3.4 Bulk resistance and bulk conductivity of Safranine O –PC composites at different concentrations.**

Concentration (ppm)	Bulk resistance (ohm)	Bulk conductivity(ohm <sup>-1</sup> cm <sup>-1</sup> )
0 ppm	8.19E+06	4.09046E-09
50 ppm	7.92E+06	4.2299E-09
100 ppm	7.69E+06	4.35642E-09
150 ppm	7.57E+06	4.42547E-09
200 ppm	7.37E+06	4.54557E-09
250 ppm	7.15E+06	4.68543E-09

### 3.8.2. Dielectric Parameters

In the present section the dielectric parameters  $\epsilon'$  and  $\epsilon''$  are studied in wide range of frequencies at room temperature. Fig.3.11 shows the variation of the dielectric constant  $\epsilon'$  and dielectric loss  $\epsilon''$  versus frequency for all concentrations of Safranine O in PC matrix. It can be noticed that  $\epsilon'$  and  $\epsilon''$  decreased with increasing frequency in the frequency range of  $\omega\tau \gg 1$  for Safranine O -PC composites. This behavior can be described by the Debye dispersion relations [Eq. (3.9) and Eq. (3.10)] [15].

$$\epsilon' = \epsilon_{\infty} + \frac{\epsilon_0 - \epsilon_{\infty}}{1 + \omega^2 \tau^2} \quad (3.9)$$

$$\epsilon'' = \frac{(\epsilon_0 - \epsilon_{\infty}) \omega \tau}{1 + \omega^2 \tau^2} \quad (3.10)$$

where  $\epsilon_0$  is the dielectric constant at low frequency,  $\epsilon_{\infty}$  is the dielectric constant at high frequency,  $\omega$  is the angular frequency, and  $\tau$  is the relaxation time.

The decrease of  $\epsilon'$  and  $\epsilon''$  with frequency can be associated to the inability of dipoles to rotate rapidly leading to a lag between frequency of oscillating dipole and that of applied field. The variation indicates that, at low frequencies; the dielectric constant is high due to the interfacial polarization and the dielectric loss ( $\epsilon''$ ) becomes very large due to ionic or molecular polarizations[16]. In addition no remarkable variation of dielectric constant or dielectric loss with Safranin O concentration which confirms that there are no changes in the polymer matrix Safranin O.

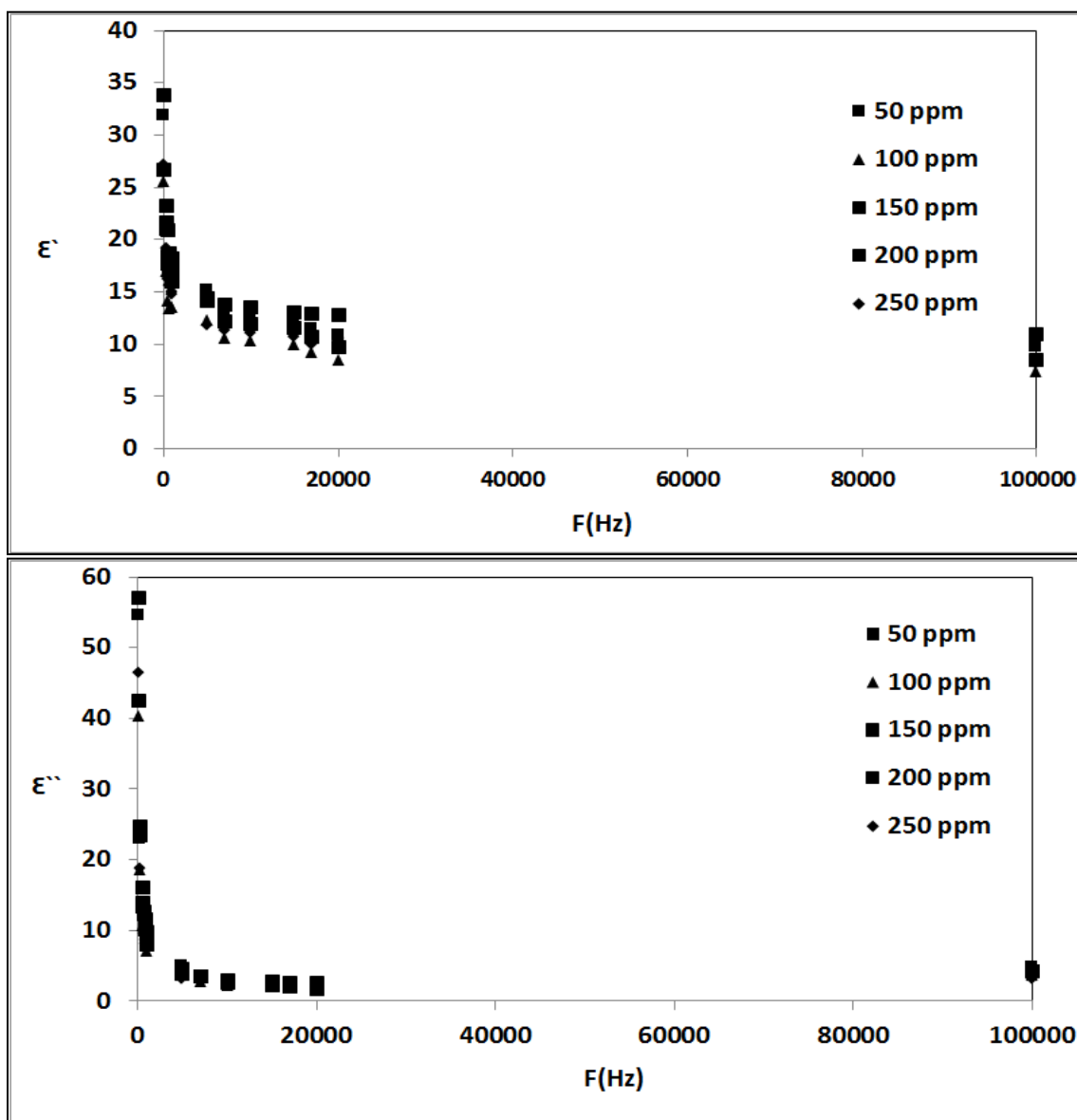


Fig. 3.11 The variation of the dielectric constant  $\epsilon'$  and dielectric loss  $\epsilon''$  versus frequency at different concentrations of Safranin O.



## **Conclusion**

From the obtained results and discussion one concludes the following: The optical absorption as well as the fluorescence peaks clearly illustrated at 518 and (564-589nm) respectively. The TGA, DSC and FT-IR did not illustrate variation for all of the following: decomposition energy around 165.5 k J/mole, melting temperature around 288 °C and glass transition temperature around 82 °C. From the above results, there is no chemical interaction between Safranin O and PC. The UV-Vis results illustrate that the optical energy gap of Safranin O –PC composite is (2.26-2.22) eV.

## References

- [1] W. D. Callister, *Materials Science and Engineering*, John Wiley & Sons, New York, 2007.
- [2] C. Espejo, A. Arribas, F. Monzo', P. P. Díez, Nano composite films with enhanced radiometric properties for greenhouse covering applications, *Journal of Plastic Film & Sheeting*, 28(4), (2012), 336–350.
- [3] M.k. Mishra, Y. Yagci, *Handbook of Vinyl Polymers radical polymerization, process, and technology*, Taylor & Francis Group, LLC, NEW YORK, 2009.
- [4] A. Ait-Kadi, M. Bousmina, A.A. Yousefi, F. Mighri, High Performance Structured Polymer Barrier Films Obtained From Compatibilized Polypropylene/Ethylene Vinyl Alcohol Blends, *polymer engineering and science*, 47, (2007), 1114-1121.
- [5] H. Becker, L. E. Locascio, review Polymer microfluidic devices, *Talanta*, 56 (2002) 267–287.
- [6] Dr. A. Seidel, *Encyclopedia of Polymer Science and Technology*, John Wiley & Sons, Inc, 111 River St., 8-01, Hoboken, NJ 07030-5774, 2014.
- [7] L. Bai, *Optical properties of CdGeAs<sub>2</sub>*, Morgantown, West Virginia, (2004).
- [8] S.M. El-Bashir, O.A. AlHarbia, M.S. AlSalhia, Optimal design for extending the lifetime of thin film luminescent solar concentrators, *Optik*, 125 (2014) 5268–5272.
- [9] S.M. El-Bashir, F.M. Barakat, M.S. AlSalhi, Metal-enhanced fluorescence of mixed coumarin dyes by silver and gold nanoparticles: Towards plasmonic thin-film luminescent solar concentrator, *Journal of Luminescence*, 143 (2013) 43–49.
- [10] B. Valeur, *Molecular Fluorescence: Principles and Applications*, Wiley-VCH Verlag GmbH, NEW YORK, 2001.
- [11] E. Ghorbel, I. Hadriche, G. Casalino, N. Masmoudi, Characterization of Thermo-Mechanical and Fracture Behaviors of Thermoplastic Polymers, *Materials*, 7, (2014), 375-398.

- [12] A. Davis, J. H. Golden, Thermal Degradation of Polycarbonate, J. Chem.Soc, B, (1968), 45-47.
- [13] S. Maitra, S. Mukherjee, N. Saha, J. Pramanik, Non-isothermal decomposition kinetics of magnesite, Cerâmica, 53 (2007), 284-287.
- [14] S. A. Mohamed, A.A. Al-Ghamdi, G.D. Sharma, M.K. El Mansy, Effect of ethylene carbonate as a plasticizer on CuI/PVA nanocomposite: Structure, optical and electrical properties, J. of Advanced Research, 5 (2014), 79-86.
- [15] V. S. Member, IAENG, D.K. Sahu, Y. S. Member, IAENG, D.C. Dhubkarya, the Effect of Frequency and Temperature on Dielectric Properties of Pure Poly Vinylidene Fluoride (PVDF) Thin Films, IMECS, 3, (2010).
- [16] H. M. El Ghanem<sup>1</sup>, S.A. Saqa'n, M. Al Saadi, S. M. Abdul Jawad, On the Electrical and Optical Properties of Polycarbonate/MnCl<sub>2</sub> Composite, Journal of Modern Physics, 2, (2011), 1553-1559.